

Full Absorption of 3rd Harmonic ECH in TCV Target Plasmas produced by 2nd Harmonic ECH and ECCD

S. Alberti, T.P. Goodmann, M.A. Henderson, A. Manini, J.-M. Moret, P. Gomez, P. Blanchard, S. Coda, O. Sauter, C. Angioni, K. Appert, R. Behn, P. Bosshard, R. Chavan, I. Condrea, A. Degeling, B.P. Duval, D. Fasel, J.-Y. Favez, I. Furno, F. Hofmann, P. Lavanchy, J. B. Lister, X. Llobet, Z. A. Pietrzyk, A. Gorgerat, P. Gorgerat, J.-P. Hogge, P.-F. Isoz, B. Joye, J.-C. Magnin, B. Marletaz, P. Marmillod, Y. Martin, A. Martynov, J.-M. Mayor, J. Mlynar, P. Nikkola, P.J. Paris, A. Perez, Y. Peysson¹, R.A. Pitts, A. Pochelon, H. Reimerdes, J. H. Rommers, E. Scavino, G. Tonetti, M. Q. Tran and H. Weisen

Centre de Recherches en Physique des Plasmas
Association EURATOM-Confédération Suisse
Ecole Polytechnique Fédérale de Lausanne
CH-1015 Lausanne, Switzerland

¹Association Euratom-CEA sur la fusion, DRFC, CEA-Cadarache, France

email address of main author: Stefano.Alberti@epfl.ch

Abstract. An experimental study of the extraordinary mode (X-mode) absorption at the third cyclotron harmonic frequency (118GHz) has been performed on the TCV Tokamak in plasmas preheated by X-mode at the second harmonic (82.7GHz). Various preheating configurations have been experimentally investigated, ranging from counter-ECCD, ECH to CO-ECCD at various power levels. Full absorption of the 470kW of injected X3 power was measured with as little as 350kW of X2-CO-ECCD preheating. The measured absorption exceeds that predicted by the linear ray tracing code TORAY by more than a factor of 2 for the CO-ECCD case. Experimental evidence indicates that a large fraction of the X3 power is absorbed by electrons in an energetic tail created by the X2-ECCD preheating.

1. Introduction

For the first time in the TCV Tokamak, plasmas have been heated using the first of three 0.5MW gyrotrons to be deployed at a frequency of 118 GHz [1], corresponding to the third harmonic EC X-mode (X3). One of the motivations for X3 ECH in TCV is the possibility of heating at densities which are inaccessible with the existing X2 ECH system, which operates at 82.7 GHz with a total power of 3MW. In the final configuration with 1.5MW of X3 heating, the launching geometry will be vertical (top launch) such that the RF beam \mathbf{k} vector will have a very shallow incidence angle on the 3rd harmonic resonant layer. Low power transmission measurements in this launching configuration have been performed by Segui et al. [2] on a target plasma with ohmic heating only. Comparison with linear ray tracing/absorption calculations, assuming a Maxwellian distribution function, have been shown to be consistent with the measurements.

In the experiment reported here, the X3 wave was launched from the low field side via one of the upper lateral launching antenna normally used for X2 heating [3]. In this launching scheme the RF beam \mathbf{k} vector has a large incidence angle on the resonance layer and therefore is favourable for interaction with a wide electron energy spectrum. These experiments were aimed at establishing the importance of plasma conditions on the absorption of X3 ECH power. For this purpose the plasmas were preheated with different power levels of X2 ECH and ECCD.

2. Experimental configuration

The target plasmas used in these experiments have the parameters $R=0.88\text{m}$, $a=0.25\text{m}$, elongation $\kappa=1.31$, $B_T = 1.42\text{T}$, $n_e(0)= 2.5 \times 10^{19}\text{m}^{-3}$. The cold resonances corresponding to the X2 and X3 frequencies are spatially separated by approximately 50mm, and, in the target plasma studied here, they are symmetric with respect to the plasma center; the X3 cold resonance being on the low field side.

The launching geometry, as well as a time trace of the relevant plasma parameters, are shown in Fig. 1. The top trace shows the time sequences for the 2nd and 3rd harmonic heating. For all launching configurations the X2 was kept at constant power from 0.3s to 1.3s whereas the X3 power was applied from 0.5s to 1.2s and included a phase with 100% modulation at 237Hz between 0.8s and 1s.

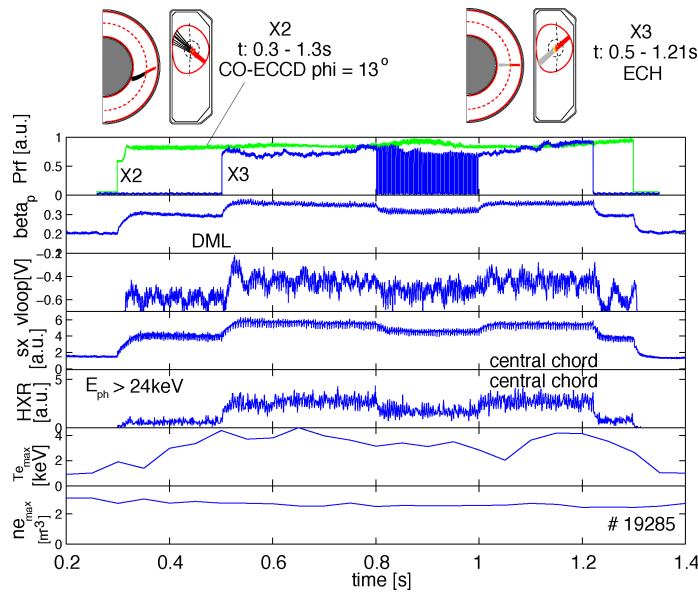


Fig. 1 Launching geometry and typical time traces for the X2 and X3 ECH. For X2, the toroidal injection angle is $\phi=13^\circ$ (CO-ECCD). From top to bottom: RF power for X2 and X3, beta poloidal measured with DML, loop voltage, soft x-ray signal (central chord), hard x-ray signal (central chord), Thomson scattering peak electron temperature and density (every 50ms).

$$P_{X2} \approx P_{X3} = 0.47\text{MW}, I_p = 200\text{kA}.$$

The large fluctuations on the central electron temperature measured by Thomson scattering are related to the sawtooth character of the plasma and the 50ms interval between Thomson measurements, the low temperature values being correlated with sawtooth crashes.

The total stored energy variation was measured during the modulated portion of the X3 RF pulse using a diamagnetic loop (DML). The modulation frequency $f_m=237\text{Hz}$ was chosen such that $1/2\pi f_m < \tau_e \sim 5\text{ms}$, where τ_e is the electron energy confinement time.

While the X3 power (0.47MW) and launching geometry, aimed at the plasma centre, were kept constant in this series of experiments, different X2 conditions were investigated including variations of the toroidal launch angle ϕ , the power deposition radius, the total X2 power and the plasma loop voltage by varying the plasma current.

3. X3 absorption measurements

All absorption measurements have been performed with the DML diagnostic in the modulated phase of the X3 power injection which provides an absolute measurement of the absorbed rf power.

Figure 2 shows the X3 absorbed power fraction, versus X2 preheat power for three X2 launching angles corresponding to central CO-ECCD ($\phi=13^\circ$), ECH ($\phi=0^\circ$) and CNT-ECCD ($\phi=-13^\circ$). For CO-ECCD target plasmas, within the experimental error bars, 100% absorption is obtained. A polarization scan of the X3 rf-beam as well as a poloidal scan of the launching

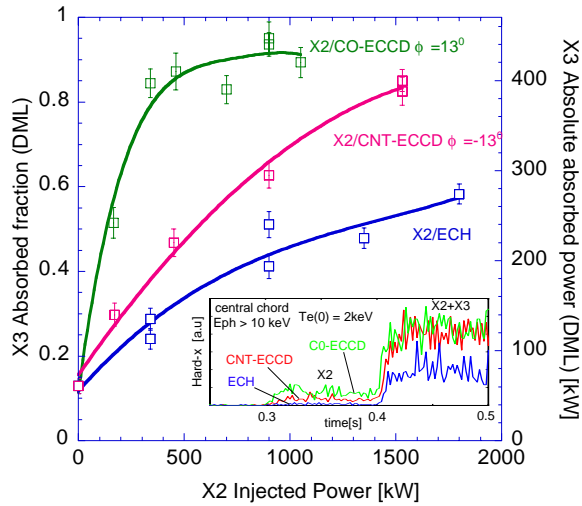


Fig. 2 Measured X3 absorption using the DML versus X2 preheat power for three different X2 launching configurations:

- CO-ECCD ($\phi=13^\circ$),
- CNT-ECCD ($\phi=-13^\circ$)
- and ECH ($\phi=0^\circ$).

The 3rd harmonic injected power was kept constant at 0.47MW with central deposition and zero toroidal injection angle (ECH).

The insert shows a comparison of the hard x-ray signal for the three launching configurations and for equal injected power of X2 and X3 (470kW)

angle (from central to off-axis) has demonstrated that single-pass absorption is measured with the DML diagnostic.

As shown in Fig. 3, a detailed toroidal injection angle scan of the X2 launch, with $P_{X2} \approx P_{X3} = 0.47\text{MW}$, has revealed a clear asymmetry in the X3 absorbed fraction. The measured X3 absorption (blue curve) is highest in a target plasma with X2 injected at a toroidal angle of $\phi=13^\circ$, corresponding to CO-ECCD. The calculated absorption with the linear ray tracing code TORAY[4] (red curve) assumes an isotropic Maxwellian distribution function.

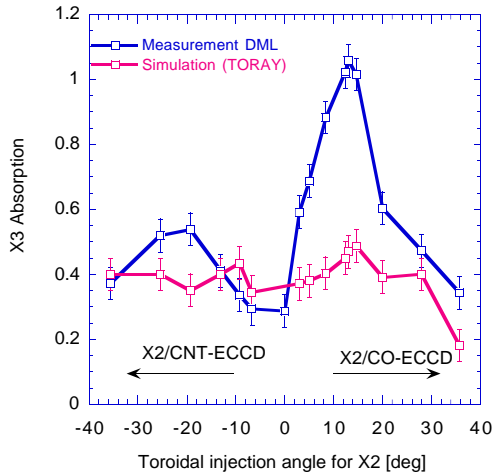


Fig. 3 Measured absorption with DML (blue curve) and calculated absorption with TORAY (red curve) versus X2 injection angle. The X2 and X3 injected power are equal at 470 kW. The TORAY code is runned using an isotropic Maxwellian distribution function.

For the largest toroidal angle in CO-ECCD ($\phi=36^\circ$), significant refraction of the X2 wave is occurring with a resulting X2 absorption of 38% only (TORAY). For all other toroidal angles, full absorption of X2 is predicted.

For this same toroidal angle scan, the variation of the plasma bulk parameters measured by Thomson scattering such as central electron temperature and density are shown in Fig. 4.

The red curves are measured during the X2 preheating phase (0.3-0.5s) while the blue curves are measured with the X3 power applied. As mentioned previously, the poor absorption of the X2 power at $\phi=36^\circ$ is consistent with the significantly lower bulk temperature already during the X2 preheating phase. The slight central density reduction once the X3 power is applied (CO- and CNT-ECCD) is due to pump out effects observed on the density profiles. The strong asymmetry in the measured absorption observed in Fig. 3 can also be seen on the bulk plasma parameters during the X3 heating. Note that this is reflected in the TORAY results (Fig. 3) but still not sufficient to account for high absorption.

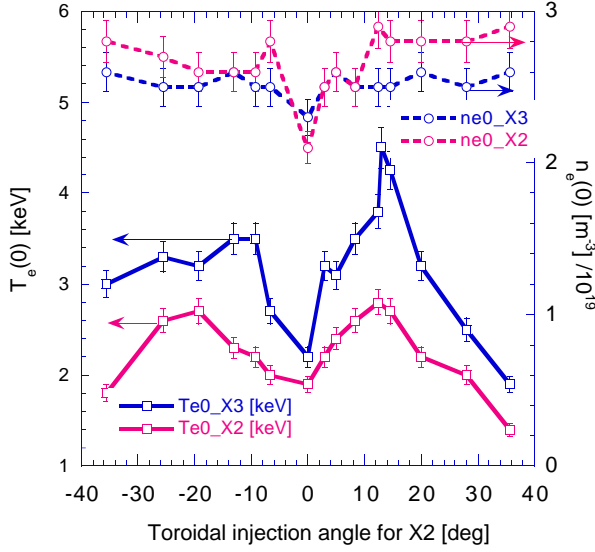


Fig. 4 Fitted central electron temperature and density measured by Thomson scattering versus toroidal injection angle. The X2 and X3 power are as in Fig. 3.

The red curves are measured during the X2 preheating phase(0.3-0.5s) while the blue curves are measured with the X3 power applied.

The Ohmic electric field effect on the X3 power absorption is shown in Fig. 5 where via a plasma current scan from 130kA to 230kA, the loop voltage was varied in the range 0.23-0.55V (green curve). With the X2 preheating in CO-ECCD at $\phi=13^\circ$, a substantial decrease in the absorption of the X3 wave is observed as the loop voltage is reduced (blue curve). Moreover, as the loop voltage is decreased, the difference between the measured absorption and the one predicted by TORAY is significantly reduced as well.

4. Discussion

Calculations of the theoretical absorption with the ray tracing code TORAY, using an isotropic, Maxwellian velocity distribution, are in fair agreement with the experimental results corresponding to ECH preheating. This observation is also in agreement with X3 absorption measurements by Pachtman et al. [5]. However, the measured X3 absorption exceeds that predicted by TORAY by a factor of up to 2 for the CNT- and CO-ECCD cases. A likely explanation of the discrepancy is that a large fraction of the X3 power is absorbed by energetic tail electrons created by X2 ECCD. The presence of these tails is confirmed by the measurement of photon spectra using an energy resolving hard x-ray camera (Figs.1 and 2 (insert)) and a high field side ECE radiometer (Fig. 6). The high-field side ECE radiometer detects suprathermal radiation levels several times larger than the thermal level, while effective x-ray photon temperatures of tens of keV are measured in the presence of ECCD. The radiometer time traces in Fig. 6 show that during the X2 preheating (0.3s<t<0.5s), no suprathermal electrons are generated for the quasi-ECH case (left figure), since the signals are

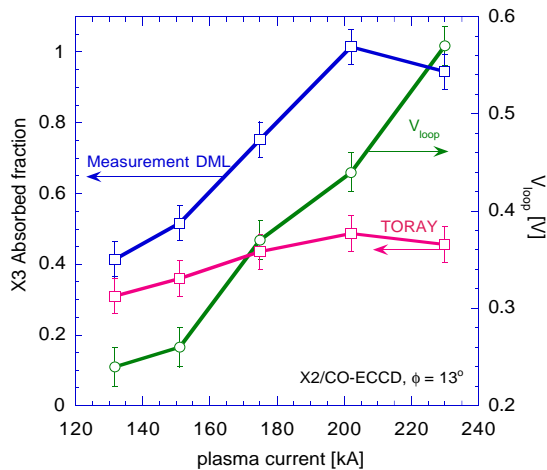


Fig. 5 Loop voltage dependence of the X3 absorption with X2 preheating in CO-ECCD at $\phi = 13^\circ$. The loop voltage scan has been performed by varying the plasma current (green curve). The blue curve is measured with the DML and the red curve gives the X3 absorption predicted by TORAY.

consistent with Thomson, on the contrary, for the CO-ECCD case, a significant deviation from Thomson is observed which indicates that a suprathermal electron tail is present. Comparing the two radiometer channels in the two cases (quasi-ECH and CO-ECCD) one can deduce that the suprathermal electrons are spatially located between the normalized minor radii $r/a = 0$ and $r/a = 0.5$ since, for the off-axis channel (red traces), the deviation from Thomson is very weak during the entire plasma discharge.

For an equal injected power of X2 and X3 (470kW), in the insert of Fig.2 a time trace of photon energies above 10keV is shown for the three different cases (CNT-ECCD, ECH, CO-ECCD). The photon counts and the ECE radiometer, are consistent in showing a weaker generation of suprathermal electrons during the ECH preheating phase.

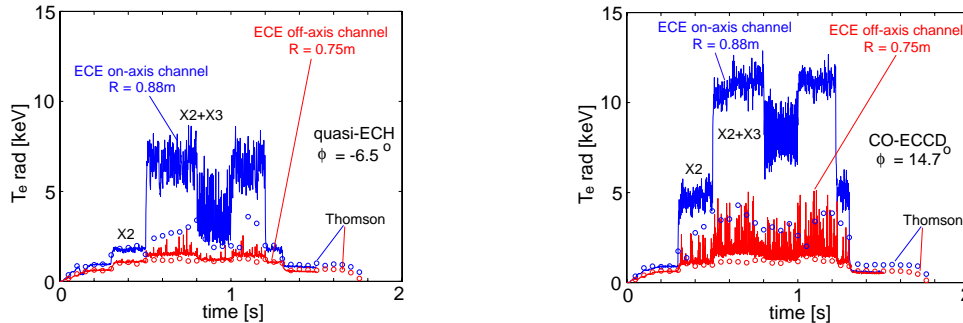


Fig. 6 Time traces of the high field-side ECE radiometer: left figure for quasi-ECH at $\phi = -6.5^\circ$ and right figure for CO-ECCD at $\phi = 14.7^\circ$. In both figures, two radiometer channels are shown: a central view ($R = 0.88m$, blue curves) and an off axis view ($R = 0.75m$, red curves). All radiometer signals have been calibrated against the Thomson scattering diagnostic (circles) during the ohmic phase ($t < 0.3s$). $P_{X2} \approx P_{X3} = 0.47MW$.

The bulk peak temperature ($T_e(0) = 2keV$) measured by Thomson scattering during the X2 preheating (0.3-0.4s) is the same for the three cases. Also, in the ECH preheating case, the weaker suprathermal electron population is spatially located in an unfavourable region for enhanced X3 absorption due to the fact that the X2 cold resonance is placed far to the high field side of the X3 resonance whereas for ECCD is shifted outward by $\approx 25mm$. Either or both of these mechanisms might explain the low absorption observed in Fig. 3 around $\phi=0^\circ$.

The toroidal angle asymmetry suggests that the Ohmic electric field plays an important role in shaping the energetic tail electron velocity distribution. This hypothesis is confirmed by ECE, hard x-ray and absorption measurements in a loop voltage scan in the range 0.23-0.55V, obtained by varying the plasma current from 130-230 kA, with $\phi=13^\circ$. Absorption decreases significantly as the loop voltage is reduced. Detailed analysis of the experimental data, as well as calculations of self-consistent distribution functions by means of a Fokker-Planck code, are in progress.

Acknowledgement: This work was partly supported by the Swiss National Science Foundation. The hard x-ray camera is on loan from the Tore Supra group (CEA,Cadarache).

References:

- [1] S. Alberti et al., to be published in Fusion Engineering Design.
- [2] J.-L. Segui et al., Nuclear Fusion, Vol. 36, No. 2 (1996).
- [3] T. P. Goodman et al., Proc. of 19th Symp. On Fusion Technology (Lisbon, 1996) vol.1 Ed. C. Varandas and F. Serra (Amsterdam: Elsevier), p 565.
- [4] A. H. Kritz et al. Proc. 3rd Varenna-Grenoble Int. Symposium on Heating in Toroidal Plasmas (Grenoble 1982) (Brussels: CEC) Vol.II, p.707.
- [5] A. Pachtman, S.M. Wolfe, I.H. Hutchinson, Nuclear Fusion, Vol.27, No.8, (1987).